MDPI

Article

Evaluation of Fire Hazard in Electrical Installations Due to Unfavorable Ambient Thermal Conditions

Seweryn Szultka [1] , Stanislaw Czapp [1],* , Adam Tomaszewski [2] and Hayat Ullah [1]

[1] Faculty of Electrical and Control Engineering, Gdansk University of Technology, Narutowicza 11/12, 80-233 Gdansk, Poland
[2] Institute of Fluid-Flow Machinery, Polish Academy of Sciences, Fiszera 14, 80-231 Gdansk, Poland
* Correspondence: stanislaw.czapp@pg.edu.pl

Abstract: Evaluation of fire hazard caused by electrical installations is a difficult and important topic, and it limits the possibility of loss of life or health of people, as well as the occurrence of significant property damage. In particular, this hazard was caused by power cables and especially photovoltaic (PV) installations. The authors proved that power cables directly exposed to strong solar radiation are likely to exceed maximum permissible temperature in unfavorable ambient conditions. Overheated and damaged cable insulation can be a source of electric shock and a strong leakage current causing fire. In the case of typical PV connectors (MC4 connectors), the main problem is poor contact at the connections of the PV cables. A poor connection can even cause the connector to melt, as shown in this study. In the paper, the authors present a computer simulation regarding critical thermal points of electrical installations, in particular, of the PV type. It may be an indication of what should be paid attention to when designing and implementing such installations. This is important for the safety of people and buildings.

Keywords: fire hazard; numerical simulations; overheating; power cables; photovoltaics

1. Introduction

The current-carrying capacity of power cables is an important operational parameter of both transmission and distribution networks. The current-carrying capacity is a measure of the power transmission of power lines, including low-voltage cable lines directly connected to electricity consumers. This capacity informs about the maximum value of the electric current flowing through the power cables, which will not cause thermal damage to the insulation as a result of exceeding the permissible temperature for a long time. The continuous increase in the demand for electricity and the increasing number of generation sources integrated with the power system, as part of renewable energy sources, result in the growing interest in the possibilities of increasing the load of power cable lines. The current-carrying capacity of power cables depends mainly on: the construction of the power cables and their arrangement and environmental conditions. The influence of each of these factors on the current-carrying capacity of conductors is defined in the IEC [1–4] and IEEE [5] standards. These standards take into account individual factors selectively and do not refer to all phenomena actually occurring in power installations. The indicated standards do not take into account, among others, the influence of: variable wind speed and direction, variable insolation, dry zones around underground power cables, as well as many other factors affecting the current-carrying capacity of conductors. The indicated standards are based on the Neher–McGrath calculation method from 1957 [6]. However, this method is not very precise [7]. Therefore, reliable knowledge of the current-carrying capacity can be obtained through experimental tests and numerical analysis. As reported in [8–10], numerical calculations of thermal states of power cables with the use of dedicated software are becoming more and more important, and the provisions of the above-mentioned standards are only used to confirm the results of simplified numerical modeling.

Knowledge of the actual operating conditions of power cables allows to avoid design errors and, as a result, will increase the reliability and safety of power installations [11,12].

The temperature of the wiring elements has a significant impact on their durability, especially their thermal endurance [13]. The authors of the referred article pointed out that there is a real risk of the wires overheating in the air, especially in the presence of direct sunlight. The authors of the paper [12] indicated the important role of the color of the roofing and the distance of the electrical installation from the roof surface. However, the impact of the indicated factors in the context of photovoltaic (PV) installations was not analyzed. The paper [14] pointed to a significant problem related to the destruction of electrical equipment (including power cables and connectors). The described destructive phenomena did not refer to the contact resistance of materials. In the article [15], it is indicated that, based on operational experience, 70% of power line failures occur in places where they are connected. This is the effect of the contact resistance and its increasing value as a result of the phenomena occurring in the contact structure, as well as the influence of external forces. In addition, a damaged electrical contact point most often causes overheating of the connector, as well as short circuits and fire. In addition, temperature is a reliable and important indicator in assessing the condition of a cable joint. In turn, the article [16] proposed a real-time temperature monitoring system for power cable joint. The proposed solution to the problem of heating the joints is suitable only for special applications. To emphasize the importance of the problem of heating up the cable connection points, GPRS wireless communication technology was also proposed [17].

Problems with the DC joints/connectors are the main cause of failure as well as fire risk in PV systems [18,19]. It is estimated that nearly 70% of all fires in PV installations are the result of improper connections in DC circuits [18]. From a scientific point of view, a potential cause of fire in PV systems due to the DC connector is the increase in its contact resistance. An equally important issue related to the fire protection of PV installations is the occurrence of possible arc faults, very often caused by bad connections. The authors of the paper [20] indicate the types and characteristics of arc faults in PV installations but do not indicate the methods of detecting such hazards. The paper [21] indicates the types of short circuits occurring in PV installations based on practical events in PV farms. The authors of the paper point out the special role of protections integrated with inverters (protection against arc faults). The article [22] provides information on the occurrence and characteristics of earth fault currents on the DC side and the related possible fire hazard of PV installations.

This article presents the influence of unfavourable environmental conditions (insolation, low wind speed) on the temperature distribution of power cables and cable connectors used in typical PV installations. The effect of contact resistance of the connections on their temperature is also investigated. The above-mentioned issues are not deeply analysed in the literature. Results of the authors' investigation show the points of electrical installations which may be a cause of the possible fire hazard as well as electric shock. Indicating these points is a key issue to prevent fires in new installations.

The rest of the paper is organized as follows. Section 2 presents an analysis of the influence of solar radiation on the current-carrying capacity and temperature of AC power cables. In Section 3, an analysis of the heating of DC connectors in theoretical and practical terms is provided. Section 4 summarizes the obtained results.

2. The Impact of Solar Radiation on the Temperature Distribution and Current-Carrying Capacity of AC Power Cables

In order to present the impact of unfavorable ambient conditions on the long-term current-carrying capacity (and thus on the temperature distribution) of power cables, a low-voltage power cable line was tested by computer simulations. The simplified model presented in Figure 1 was implemented in a 3-D numerical model in the ANSYS Fluent software.
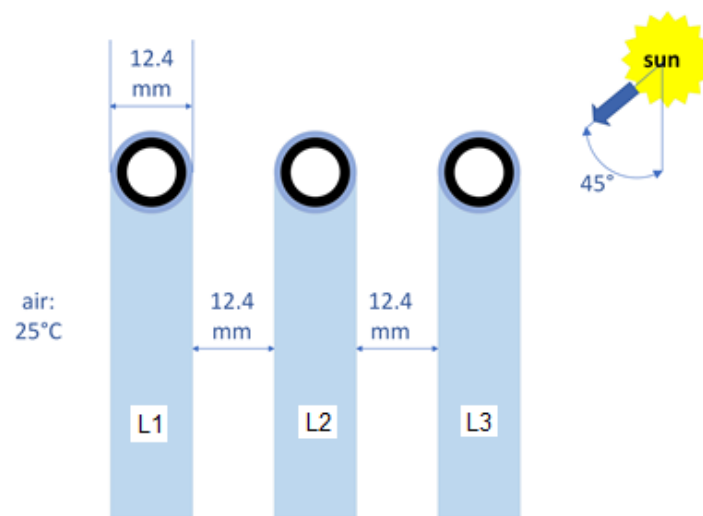
Figure 1. The analyzed power cable line composed of three single-core cables.

Figure 1 shows a power cable line laid vertically in air at a temperature of 25 °C. The given air temperature corresponds to Polish climatic conditions in accordance with the standard [3]. Three power cables (three-phase alternating current line of nominal frequency 50 Hz) with a cross-sectional area of 35 mm^2 with a conductor made of copper and insulation and a sheath made of PVC are arranged with a spacing equal to the diameter of the power cable.

In the numerical model, all heat exchange mechanisms involved in the real system were introduced:

- Joule's heat—generated by the flow of electric current,
- solar radiation heat,
- convection heat,
- dissipated radiation heat.

In order to investigate the effect of the real conditions of cables heating, the heat of solar radiation falling at an angle of 45° on the cable surface (conditions typical for Europe), convective air movement and a radiation model according to the discrete ordinates theory were modeled. An example of a computational mesh in a cross section is shown in Figure 2.
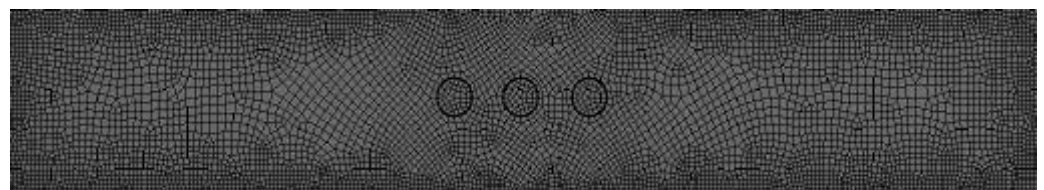

Figure 2. A view showing the numerical grid for power cable temperature estimation.

The total number of mesh elements was approximately 9 million finite volumes. The results of particular calculation variants are presented in the further part of the article. A steady-state simulation was performed and turbulence model k-epsilon was chosen. The proper materials were set in the model in certain cell zones and the boundary conditions were as follows:

- mass flow inlet (bottom side of domain),
- pressure outlet (upper side of domain),
- mesh interfaces between different cell zones,
- heatflux (the inner side of power cables),
- heatflux (external side of power cables, which is exposed to solar radiation).

In the case of heating the cable line in accordance with the presented assumptions and in the absence of electric current flow, the temperature distribution around the cables was obtained as shown in Figure 3.
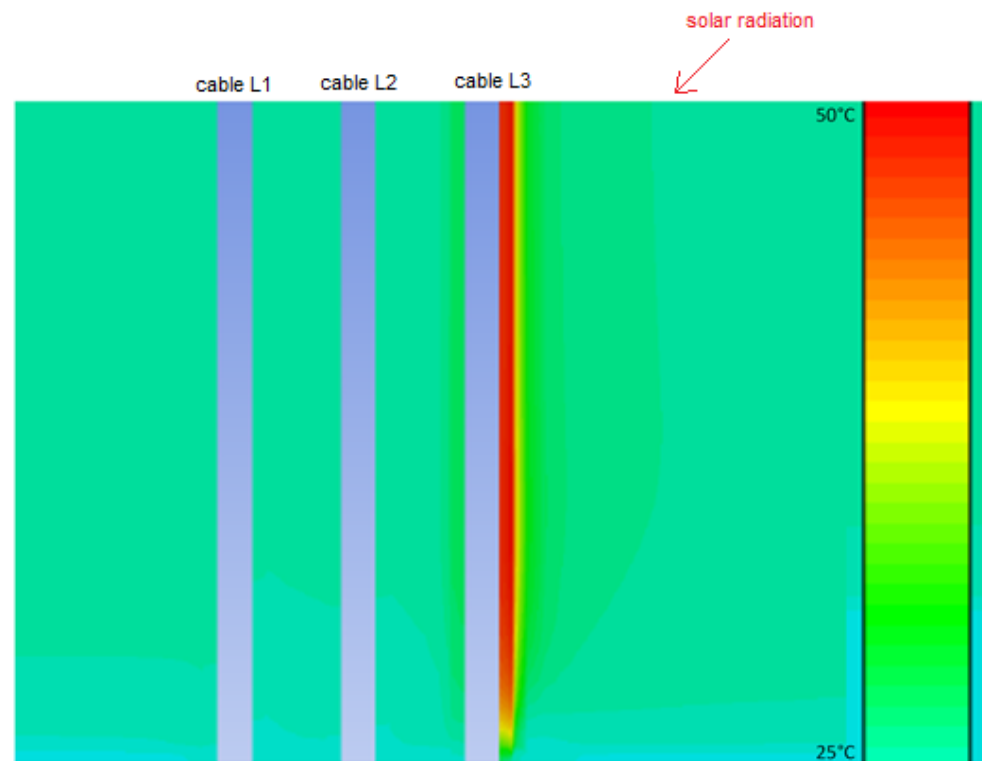

Figure 3. Temperature distribution around unloaded power cables ($I_Z = 0$ A) taking into account solar radiation (close-up view of the cables).

In the analyzed model, Figure 3 shows the effect of solar radiation alone (without current load) on the temperature of the power cable especially in the L3 phase (cable on the right). Taking into account the solar radiation and the lack of current load on the cables, the cable insulation temperature in the L3 phase reaches 50 °C. Thus, the solar radiation increased the temperature of the power cable insulation by 25 °C (from ambient temperature equal to 25 °C).

Figure 4 shows the temperature distribution around power cables which are symmetrically loaded and unaffected by solar radiation. The current-carrying capacity of the cable system is equal to 152 A. The current value was achieved by iteratively increasing the Joule's heat in the conductor until the permissible temperature (70 °C for PVC insulation) was reached.

Figure 5 shows the temperature distribution around power cables which are symmetrically loaded and under the influence of solar radiation. The current-carrying capacity of each power cable is 96 A. The current value was determined on the basis of computer calculations—in the assumed conditions it obtains the max temperature of the cable insulation equal to 70 °C (max permissible).

Comparing the simulation results presented in Figures 4 and 5, one can notice a significant decrease in the current-carrying capacity of power cables due to the impact of solar radiation. As a result of the influence of the heat of solar radiation, the current-carrying capacity of power cables decreased by nearly 37%. If the need to reduce the load of the power cables is not taken into account (the cables would be loaded with 152 A instead of 96 A), the permissible temperature could be locally exceeded, which results in a reduction in insulation durability [13]. Significant overheating of the cables and damage to the insulation may also cause significant leakage current and, consequently, risk of electric shock or fire.
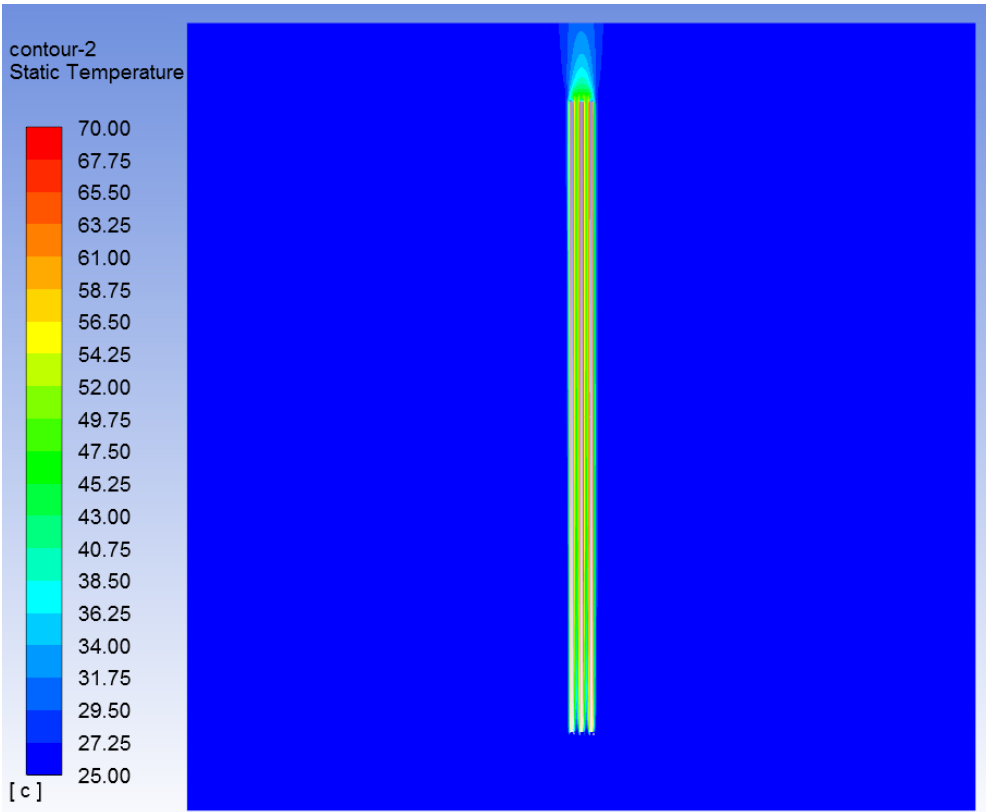
Figure 4. Temperature distribution around power cables (max permissible load: $I_{ZL1} = I_{ZL2} = I_{ZL3} = 152$ A) without solar radiation.
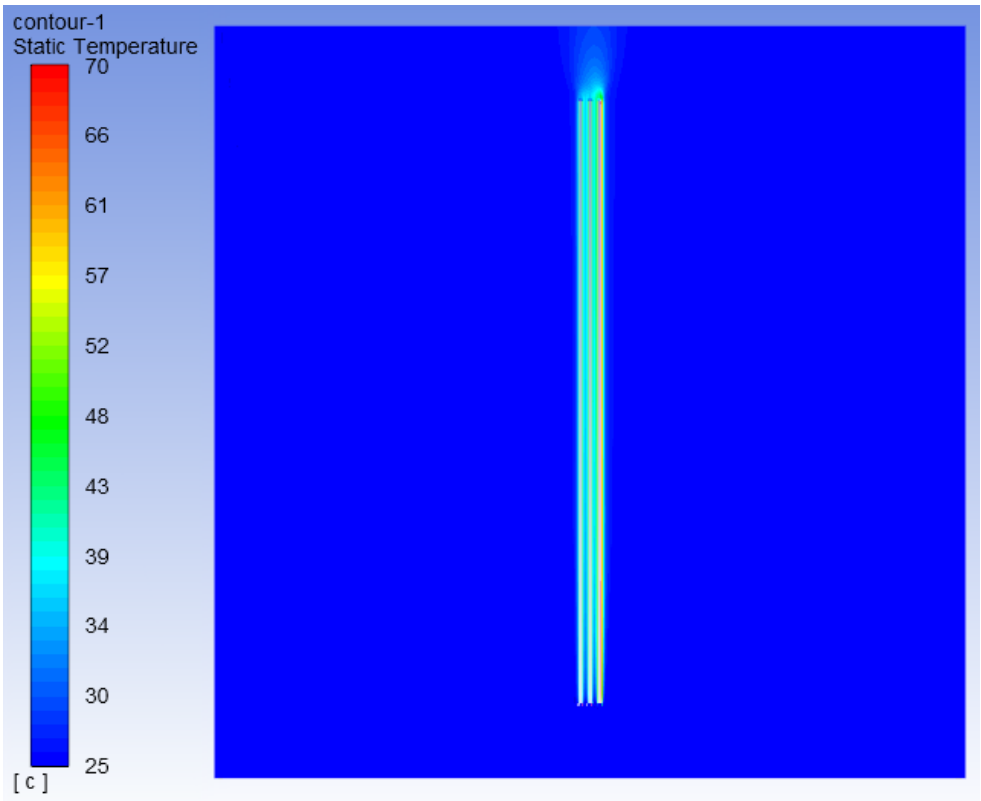

Figure 5. Temperature distribution around power cables (max permissible load: $I_{ZL1} = I_{ZL2} = I_{ZL3} = 96$ A) taking into account solar radiation.

3. The Impact of Solar Radiation and Quality of Connections on Temperature Distribution in DC Connectors

Several simulations were carried out to assess the effect of insolation and contact resistance on the temperature of DC connectors used in PV systems. For this purpose, the DC connector, commonly known as the MC4 connector, was the subject of the analysis. The connector model shown in Figure 6 has been performed in accordance with the manufacturer's catalog card [23]. The numerical approach was very similar to the one presented for the power cables in previous section. The only significant difference is that the "Solar calculator" option was set in the model instead of implementing the additional heatflux zone to simulate solar radiation. Moreover, we only consider DC flow. The computational model includes a constant value of solar radiation intensity (1200 W/m^2), an ambient temperature of 30 °C (assumed by the authors' free air temperature during a hot day in Polish climatic conditions), and low convection air movement (0.4 m/s). The parameters of the model are to reflect unfavorable heat exchange conditions in the summer months on the roof [24]. Other important simulation parameters are: connector material (polyamide), absorptivity material (0.9), and DC wire resistance (6.1 mΩ/m). It was assumed that the contact resistance between the connectors and the connected wires (resulting from the quality of cable assembly) is neglected.
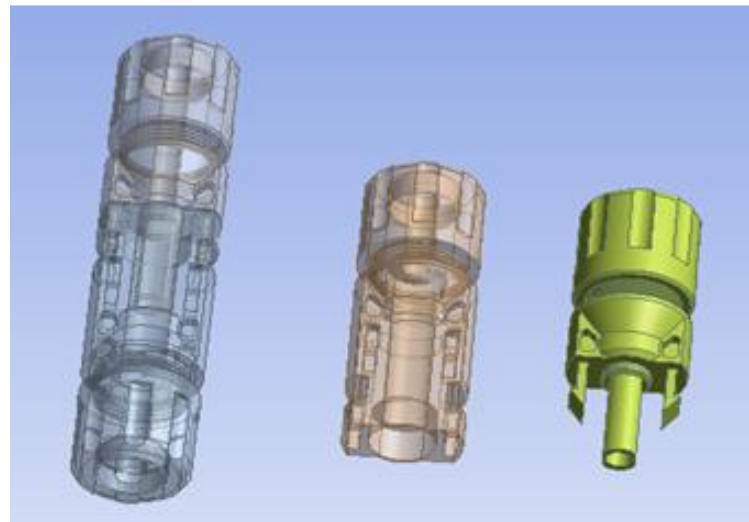

Figure 6. Analyzed MC4 connectors (simulation with ANSYS).

In the first stage of the investigation, the effect of solar radiation on the heating of the MC4 connector, without the flow of electric direct current, was examined. Figure 7 shows the heating effect of the DC connector only under the influence of solar radiation. According to the obtained simulations, the DC connector reaches a maximum temperature of 55 °C.

Then, the conditions of heat exchange with the environment with the participation of solar radiation and nominal operating conditions were examined (Figure 8).

The distribution of temperature presented in Figure 8 shows relatively good conditions for heat dissipation to the environment. Despite the flow of electric current with an assumed typical value for the connector (15 A), the increase in the temperature of the connector is recorded in the range of 6 degrees Celsius compared with no load (Figure 7). It is worth noting that the result of the temperature distribution in Figure 8 was obtained for the contact resistance respected by the manufacturer (max. 0.25 mΩ) and the rated contact force of 50 N.
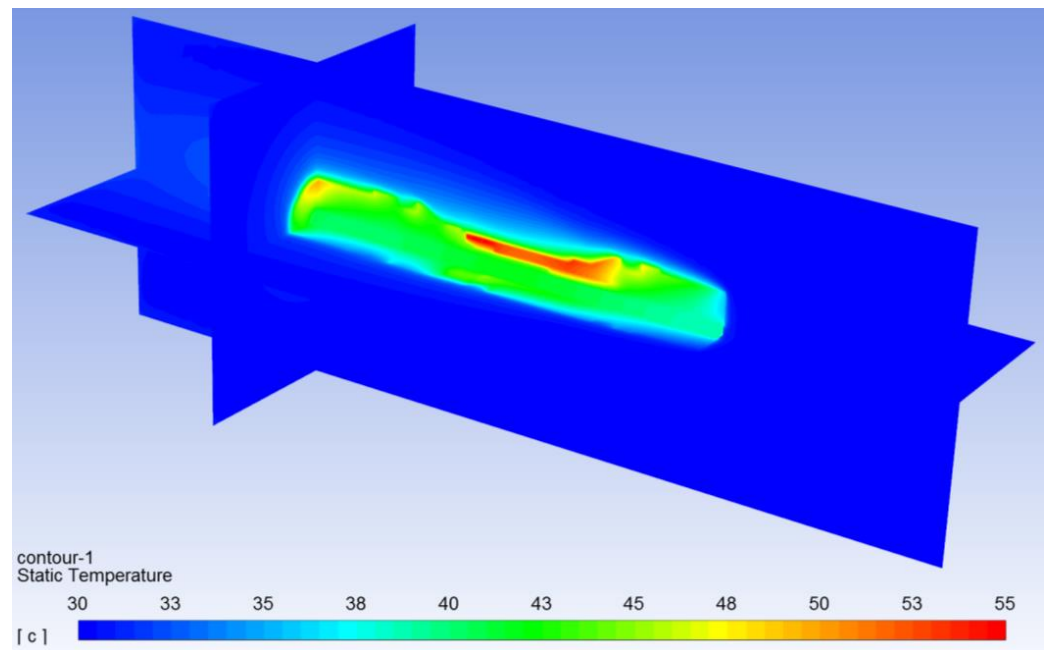
Figure 7. Temperature distribution around DC connector without current flow (*I* = 0 A) and with solar radiation. Max temperature: 55 °C.
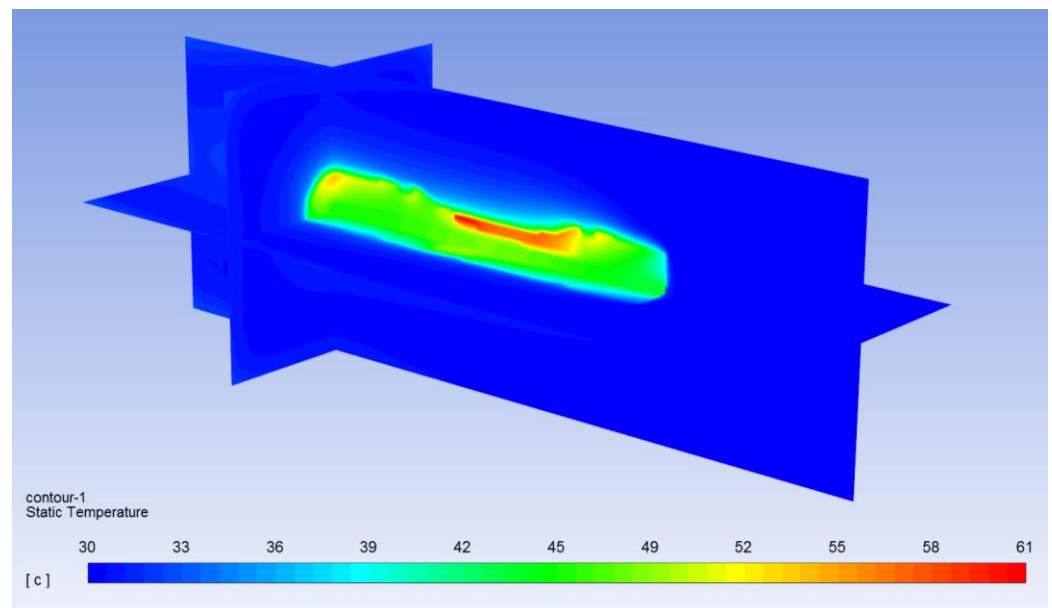

Figure 8. Temperature distribution around DC connector with current flow (*I* = 15 A) and solar radiation. Max temperature: 61 °C.

As mentioned in the first part of the article, a significant fire hazard from a DC connector can be caused by an increase in its contact resistance above the values allowed by the manufacturer. To investigate this effect, possible contact resistance values were determined depending on the contact force, based on the following equation:

$$R_P = \frac{c \cdot \rho}{(0,1F_k)^m} \tag{1}$$

where:

R_P—contact resistance, mΩ,

C— constant dependent on the contact area, -,

ρ—contact material resistivity, Ωm,

F_k—contact force, N,

m—constant depending on the type of contact, -.

According to the information contained in [25], for the contact material of which the DC connector is made (tin-plated copper), the value of the $c \cdot \rho$ coefficient (the product of constant dependent on the contact area and contact material resistivity) is equal to 1. The value of the constant m is equal to 1 (the contact of the planes). The list of calculated contact resistance values R_p depending on the contact force F_k is provided in Table 1.

Table 1. Calculated contact resistance values R_p depending on the contact force F_k.

No./Case	F_k, N	R_p, mΩ	I, A
1	50	0.2	15
2	40	0.25	14.98
3	30	0.33	14.97
4	20	0.5	14.94
5	10	1	14.85
6	1	10	13.22
7	0.5	20	11.4
8	0.3	33.33	9

The results contained in Table 1 show the value of the calculated contact resistance depending on the decreasing value of the contact force (values lower than the nominal contact force).

In the analyzed DC circuit, the current value decreases with increasing resistance—this phenomenon is taken into account for values included in Table 1. Importantly, the results presented in the first and second cases of Table 1 are consistent with the manufacturer's data. The reduced contact forces shown in Table 1 are the forces that actually occur in PV installations due to poor wiring. The presented Equation (1) assumes the averaged values of the contact coating resistance. It should be emphasized that in the case of favorable corrosion conditions of the connectors (especially moisture ingress), the coating resistance value is significantly increased.

Figures 9–11 show the temperature distribution around the DC connector, for various values of the contact resistance and the flowing electric current (cases 6, 7, and 8 from Table 1).

As the contact resistance increases, the maximum DC connector temperature also increases. It is worth emphasizing that, according to the manufacturer's card, the upper temperature limit of the connector is equal to 105 °C. Therefore, in the cases shown in Figures 9–11, this temperature has been exceeded, which results in a reduction in the durability of the connector, its possible change in structure, and possible loss of insulating properties. A summary of the calculation results of the connector heating, depending on the contact resistance, is shown in Figure 12.

The graph presented in Figure 12 refers to the data provided in Table 1. The temperature of the DC connector increases with the increase in contact resistance R_p. A significant increase in temperature is observed, in particular, for the initial increases in contact resistance (up to 1 Ω). The presented effects of excessive heating of the DC connector constitute a real fire hazard due to the possible generation of minimal ignition energy for the dust–air mixture or other diffusing mixtures present in the vicinity of the PV installation [26]. In a typical PV system, there are many DC connection points made by a set of connectors (plug-socket). If one of these connections is poorly made, it will deteriorate during operation as a result of increased contact resistance: this place heats up when current flows and a "hot spot" occurs. Due to the appearance of heat, the contact material may diffuse or even melt until, at some point, the connection will be completely broken. In this case, an arc can form over a very small air gap, resulting in a fire hazard [27]. The described occurrence of hot

spots of connectors is not only a theoretical problem—it occurred in practice, as shown in Figure 13.
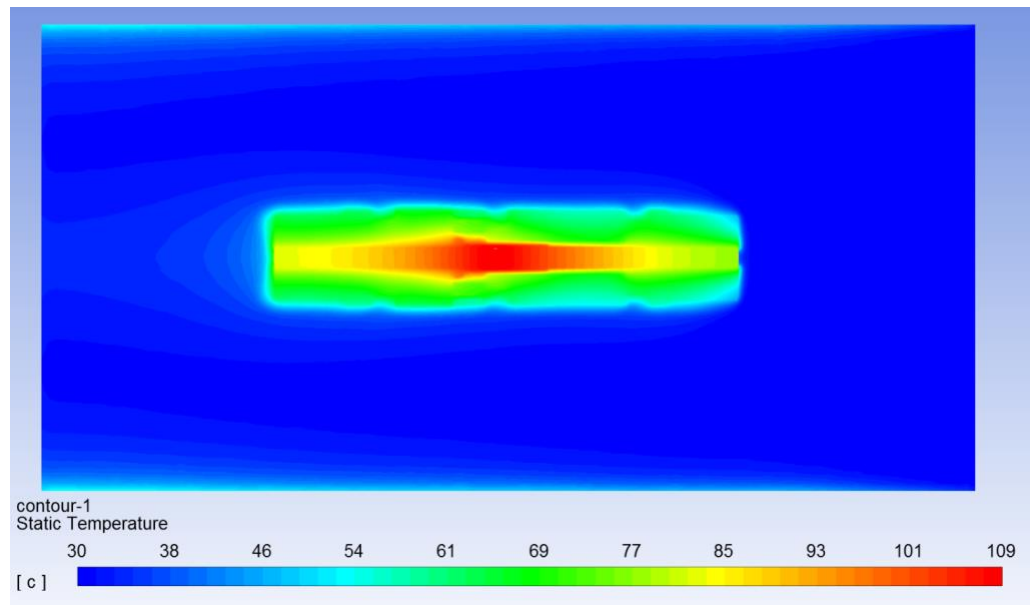

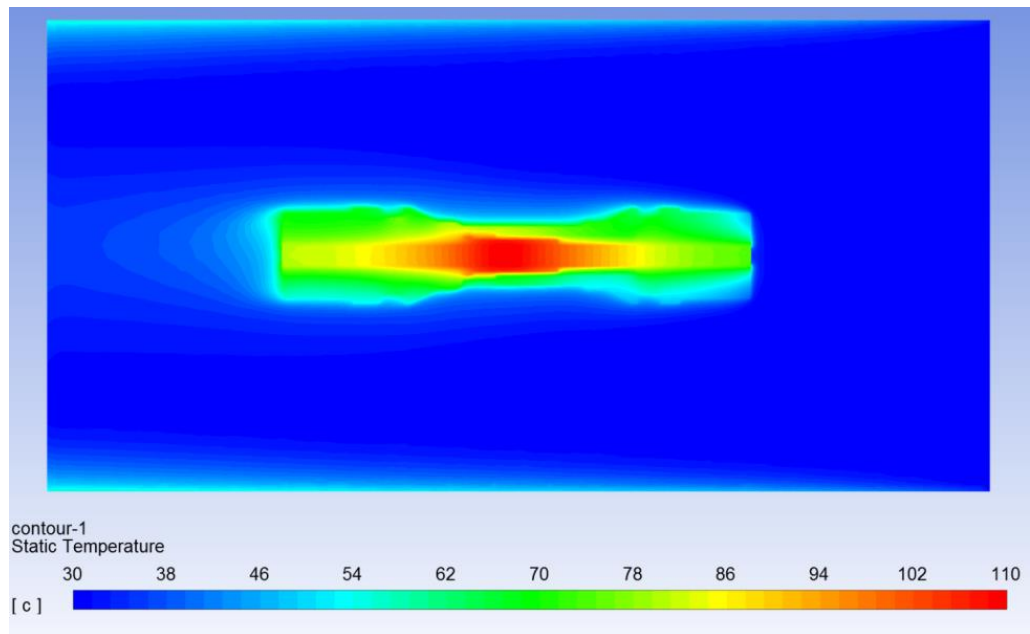**Figure 9.** Temperature distribution around DC connector with current flow (*I* = 13.22 A)—case 6 in Table 1. Max temperature: 109 °C.

Figure 10. Temperature distribution around DC connector with current flow (*I* = 11.4 A)—case 7 in Table 1. Max temperature: 110 °C.
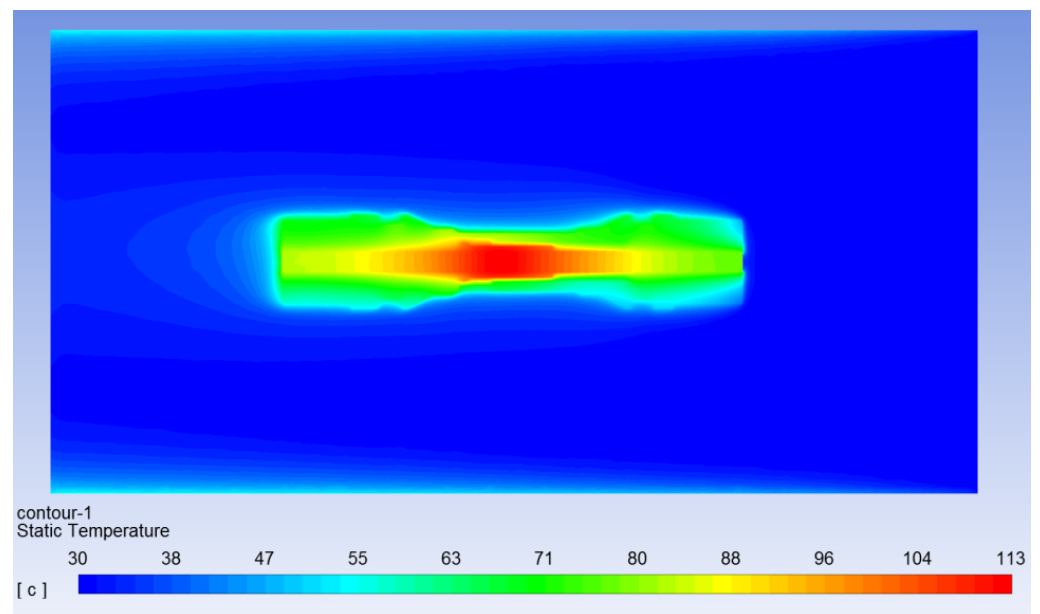
Figure 11. Temperature distribution around DC connector with current flow ($I = 9$ A)—case 8 in Table 1. Max temperature: 113 °C.
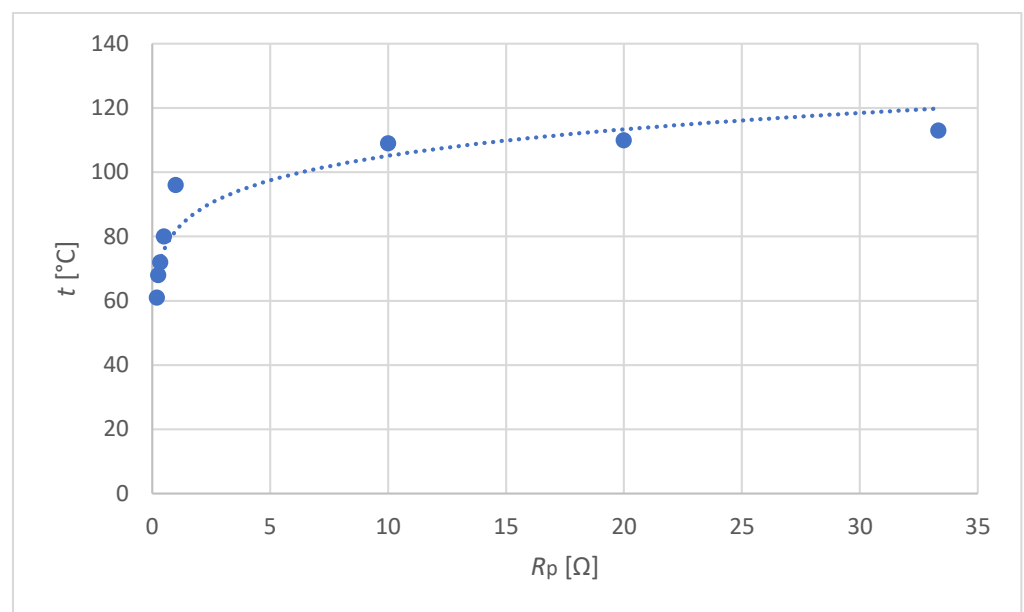

Figure 12. The dependence of the temperature of the DC connector on the value of its contact resistance.

The DC connector on the left in the photo (Figure 13) is new and unused. The connector on the right in the photo comes from a real PV installation, where the contact resistance increased above the nominal value as a result of the power cables being stretched during power generation. Finally, part of the insulation of the connector melted, which can be seen in Figure 13. This effect can also cause a fire hazard.

Figure 13. Comparison of the shape of MC4 connectors—the connector on the left is fully functional and the connector on the right is damaged due to overheating.

4. Conclusions

Currently, PV installations are very common, both as big power plants and micro-installations. Micro-installations coupled with residential buildings are a potential fire hazard, especially due to the careless mounting of these installations. As it results from the simulation tests contained in this article, both strong insolation of the wires and their poor connections may cause a significant increase in the temperature of the elements of the electrical installation. The temperature of PV DC connectors can reach 113 °C—it exceeds the value allowed by the manufacturer, which is indicated at 105 °C. A significant increase in the temperature of the PV connector occurs in the range of small contact resistance values (initial increases, up to 1 Ω)—see Figure 12.

A significant increase in temperature may lead to damage to the insulation of wires/connectors, and thus increase the risk of fire and the risk of electric shock for those in contact with these elements. Cable insulation exposed to solar radiation can heat up to 50 °C (without current load), and designers usually assume it is only 25 °C. A current load can therefore lead to the overheating of this insulation.

The results of simulation tests indicate critical points of installations, in particular PV ones, and may be a recommendation of what should be paid attention to when de-

signing and implementing such installations. This is important for the safety of people and buildings.

Author Contributions: Conceptualization, S.C. and S.S.; methodology, A.T. and S.S.; validation, S.C., A.T. and S.S.; formal analysis, S.C. and S.S.; investigation, A.T. and S.S.; resources, S.C. and S.S.; data curation, S.C., A.T. and S.S.; writing—original draft preparation, A.T. and S.S.; writing—review and editing, H.U., S.C., and A.T.; visualization, A.T. and S.S.; supervision, S.C.; project administration, S.C. and S.S. All authors have read and agreed to the published version of the manuscript.

Institutional Review Board Statement: Not applicable.

Informed Consent Statement: Not applicable.

Data Availability Statement: Data is contained within the article.

Conflicts of Interest: The authors declare no conflict of interest.

References

1. *IEC 60287-1-1:2001*; Electric Cables–Calculation of the Current Rating–Part 1-1: Current Rating Equations (100% load factor) and Calculation of Losses–General. International Electrotechnical Commission: Geneva, Switzerland, 2001.
2. *IEC 60287-2-1:2001*; Electric Cables–Calculation of the Current Rating–Part 2-1: Thermal Resistance–Calculation of the Thermal Resistance. International Electrotechnical Commission: Geneva, Switzerland, 2001.
3. *IEC 60287-3-1:1999*; Electric Cables–Calculation of the Current Rating–Part 3-1: Sections on Operating Conditions–Reference Operating Conditions and Selection of Cable Type. International Electrotechnical Commission: Geneva, Switzerland, 1999.
4. *IEC 60364-5-52:2009*; Low-Voltage Electrical Installations–Part 5-52: Selection and Erection of Electrical Equipment–Wiring Systems. International Electrotechnical Commission: Geneva, Switzerland, 2009.
5. IEEE 835: POWER CABLE AMPACITY TABLES, 1994. Publisher: Institute of Electrical & Electronics Engineers.
6. Neher, J.H.; McGrath, M.H. The calculation of the temperature rise and load capability of cable systems. *AIEE Trans.* **1957**, *76*, 752–772. [CrossRef]
7. Boron, S. Current-carrying capacity of mining flexible cables at intermittent and short-time duty. *Syst. Support. Prod. Eng.* **2017**, *6*, 21–30.
8. Holyk, C.; Anders, G.J. Power cable rating calculations—A historical perspective. *IEEE Ind. Appl. Mag.* **2015**, *21*, 6–64. [CrossRef]
9. Plesca, A.; Scintee, A. Thermal Aspects Related to Power Assemblies. *Adv. Electr. Comput. Eng.* **2010**, *10*, 23–27. [CrossRef]
10. Czapp, S.; Czapp, M.; Szultka, S.; Tomaszewski, A. Ampacity of power cables exposed to solar radiation–recommendations of standards vs. CFD simulations. *E3S Web Conf.* **2018**, *70*, 111–112. [CrossRef]
11. Spyra, F. External factors influence on current-carrying capacity in an electric power cable line. *Energetyka* **2007**, *6–7*, 451–454.
12. Brender, D.; Lindsey, T. Effect of rooftop exposure in direct sunlight on conduit ambient temperatures. In Proceedings of the IEEE Industry Applications Conference Forty-First IAS Annual Meeting, Tampa, FL, USA, 8–12 October 2006; pp. 705–711. [CrossRef]
13. Czapp, S.; Szultka, S.; Ratkowski, F.; Tomaszewski, A. Risk of power cables insulation failure due to the thermal effect of solar radiation. *Eksploat. Niezawodn. Maint. Reliab.* **2020**, *22*, 232–240. [CrossRef]
14. Paul, S.; Costea, A. Independent thermal protection for electrical circuit breaker panels, electrical power cables and lines. A practical solution proposal. In Proceedings of the 9th International Conference on Electronics, Computers and Artificial Intelligence (ECAI), Targoviste, Romania, 29 June–1 July 2017; pp. 1–5. [CrossRef]
15. Luo, H.; Cheng, P.; Liu, H.; Kang, K.; Yang, F.; Yang, Q. Investigation of contact resistance influence on power cable joint temperature based on 3-D coupling model. In Proceedings of the IEEE 11th Conference on Industrial Electronics and Applications (ICIEA), Hefei, China, 5–7 June 2016; pp. 2265–2268. [CrossRef]
16. Wenzhi, C.; Xiaohui, H.; Zhendong, G.; Chengrong, L. The design of temperature monitoring system for power cable joint. In Proceedings of the IEEE International Conference on Condition Monitoring and Diagnosis, Bali, Indonesia, 23–27 September 2012; pp. 671–676. [CrossRef]
17. Wang, W.; Wang, L.A. temperature remote monitoring system of cable joint. In Proceedings of the 2nd International Conference on Signal Processing Systems, Dalian, China, 5–7 July 2010; pp. 690–694. [CrossRef]
18. Czaja, P. Bezpieczeństwo pożarowe instalacji fotowoltaicznych. *Przeglad Elektrot.* **2021**, *97*, 105–108. [CrossRef]
19. SOLWIS Home Page. Available online: https://uzgodnienia-ppoz.online/nie-ma-kompatybilnych-zlaczek-solarnych (accessed on 5 December 2022).
20. Strobl, C.; Meckler, P. Arc Faults in Photovoltaic Systems. In Proceedings of the 2010 Proceedings of the 56th IEEE Holm Conference on Electrical Contacts, Charleston, SC, USA, 4–7 October 2010; pp. 1–7. [CrossRef]
21. Khorshed Alam, M.; Khan, F.; Johnson, J.; Flicker, J. A Comprehensive Review of Catastrophic Faults in PV Arrays: Types, Detection, and Mitigation Techniques. *IEEE J. Photovolt.* **2015**, *5*, 982–997. [CrossRef]

22. Falvo, M.C.; Capparella, S. Safety issues in PV systems: Design choices for a secure fault detection and for preventing fire risk. *Case Stud. Fire Saf.* **2015**, *3*, 1–16. [CrossRef]

23. Stäubli Web Site. Available online: https://www.staubli.com/content/dam/spot/SOL-Main-11014092-en.pdf (accessed on 15 December 2022).

24. Nominal Operating Cell Temperature. Available online: https://www.pveducation.org/pvcdrom/modules-and-arrays/nominal-operating-cell-temperature (accessed on 17 December 2022).

25. Książkiewicz, A. Electrode Processes in Low Voltage Alternating Current Relays. Ph.D. Thesis, Poznan University of Technology, Poznan, Poland, 2016.

26. Jaskółowski, W. Threats connected with combustion of cable insulation. *Elektroinfo* **2015**, *5*. Available online: https://www.elektro.info.pl/artykul/ochrona-ppoz/59537,zagrozenia-powstajace-przy-spalaniu-izolacji-kabli-lub-przewodow-elektrycznych (accessed on 18 December 2022).

27. Fronius Home Page. Available online: https://www.forum-fronius.pl/ograniczenie-ryzyka-wystapienia-pozaru-w-instalacjach-pv/ (accessed on 20 December 2022).